Structural Engineering and Mechanics, Vol. 7, No. 5 (1999) 473-484
DOI: http://dx.doi.org/10.12989/sem.1999.7.5.473

Thermal buckling analysis of thick anisotropic composite plates by finite strip method

M.S. Cheung †

Department of Civil Engineering, University of Ottawa, Ottawa, Ontario, K1N 9B4, Canada

G. Akhras ‡

Department of Civil Engineering, Royal Military College of Canada, Kingston, Ontario, K7K 5L0, Canada

W. Li ‡†

Department of Civil Engineering, Carleton University, Ottawa, Ontario, K1S 5B6, Canada

Abstract. In the present study, the thermal buckling analysis of thick anisotropic laminated composite plates is carried out using the finite strip method based on the higher-order shear deformation theory. This theory accounts for the parabolic distribution of the transverse shear strains through the thickness of the plate and for zero transverse shear stresses on the plate surfaces. Therefore, this theory yields improved results over the Mindlin plate theory and eliminates the need for shear correction factors in calculating the transverse shear stiffness. The critical temperatures of simply supported rectangular cross-ply and angle-ply composite laminates are calculated. The effects of several parameters, such as the aspect ratio, the length-to-thickness ratio, the number of plies, fibre orientation and stacking sequence, are investigated.

Key words: thermal buckling; composite plate; finite strip method.

1. Introduction

Some composite plate structures in aircrafts and space vehicles have experienced thermal buckling due to aerodynamic and solar radiation heating. Seeking a better understanding on the thermal buckling behavior of composite plates and creating more accurate and more efficient methods to predict the critical thermal buckling temperature have become an important target for many engineers and researchers. Some results have been reported (see e.g., Whitney and Ashton 1971, Stavsky 1975, Tauchert and Huang 1986, Chen and Chen 1987, Shu and Sun 1994).

In the present study, the thermal buckling analysis of thick anisotropic laminated composite plates is carried out using the finite strip method based on the higher-order shear deformation

† Professor
‡ Adjunct Professor
‡† Research Engineer

theory developed by J.N. Reddy (see Reddy 1984, Reddy and Phan 1985). This theory accounts for the parabolic distribution of the transverse shear strains through the thickness of the plate and for zero transverse shear stresses on the plate surfaces. Therefore, this theory yields improved results over the Mindlin plate theory and eliminates the need for shear correction factors in calculating the transverse shear stiffness. As indicated by Reddy, this theory can be used to simulate global behaviors (deflection, natural frequency and buckling load) for very thick plates with the length-to-thickness ratio as low as a/h=4.0. The results are satisfactory in comparison with three dimensional elasticity analysis and the extra cost in the analysis is little. Furthermore, the finite strip method is employed for the numerical implementation of the current analysis. This method utilizes a series of beam eigenfunctions to express the displacement variations in the longitudinal direction of a plate (see Cheung *et al.* 1996). Thus, the two dimensional analysis is transformed into one dimensional. The cost of analysis is reduced significantly not only due to the reduction in the required computer time and storage space, but also due to the substantial simplification of input data preparation. Moreover, the accuracy of analysis is also improved, particularly for the highly anisotropic laminates, because the numerical error attributed to the material anisotropy is also cut down by the considerable decrease in the number of unknowns involved in each analysis.

The critical temperatures of simply supported rectangular cross-ply and angle-ply composite laminates are calculated. The effects of several parameters, such as the aspect ratio, the length-to-thickness ratio, the number of plies, fibre orientation and stacking sequence, are investigated.

2. Material properties of lamina

A laminate is manufactured from orthotropic layers (or plies) of preimpregnated unidirectional fibrous composite materials. Neglecting σ_3, for each layer, the stress-strain relations in the fiber-fixed local coordinate system can be stated as

$$\begin{Bmatrix} \sigma_1 \\ \sigma_2 \\ \tau_{12} \\ \tau_{23} \\ \tau_{31} \end{Bmatrix} = \begin{bmatrix} Q_{11} & Q_{12} & 0 & 0 & 0 \\ Q_{12} & Q_{22} & 0 & 0 & 0 \\ 0 & 0 & Q_{66} & 0 & 0 \\ 0 & 0 & 0 & Q_{44} & 0 \\ 0 & 0 & 0 & 0 & Q_{55} \end{bmatrix} \begin{Bmatrix} \varepsilon_1 - \alpha_1 \Delta T \\ \varepsilon_2 - \alpha_2 \Delta T \\ \gamma_{12} \\ \gamma_{23} \\ \gamma_{31} \end{Bmatrix} \tag{1}$$

where the subscripts 1 and 2 are respectively the fiber and the normal to fibre inplane directions, 3 is the direction normal to the plate; α_1 and α_2 are the coefficients of thermal expansion; ΔT is the temperature rise from the state free of any thermal stresses; Q_{ij} are the reduced stiffness components, which can be evaluated from the experimentally determined material properties as follows:

$$Q_{11} = \frac{E_1}{1 - \nu_{12}\nu_{21}}; \quad Q_{22} = \frac{E_2}{1 - \nu_{12}\nu_{21}}; \quad Q_{12} = \nu_{12} Q_{22}$$

$$Q_{66} = G_{12}; \quad Q_{44} = G_{23}; \quad Q_{55} = G_{31}; \quad \nu_{21} = \nu_{12} E_2 / E_1 \tag{2}$$

in which E_1 and E_2 are the Young's moduli; ν_{12} and ν_{21} are the Poisson's ratio; G_{12}, G_{23} and G_{31} are the shear moduli.

By performing a coordinate transformation (see Agarwal and Broutman 1980), the stress strain relations in the global x-y-z coordinate system can be obtained as

$$\begin{Bmatrix} \sigma_x \\ \sigma_y \\ \tau_{xy} \\ \tau_{yz} \\ \tau_{zx} \end{Bmatrix} = \begin{bmatrix} Q'_{11} & Q'_{12} & Q'_{16} & 0 & 0 \\ Q'_{12} & Q'_{22} & Q'_{26} & 0 & 0 \\ Q'_{16} & Q'_{26} & Q'_{66} & 0 & 0 \\ 0 & 0 & 0 & Q'_{44} & Q'_{45} \\ 0 & 0 & 0 & Q'_{45} & Q'_{55} \end{bmatrix} \begin{Bmatrix} \varepsilon_x - \alpha_x \Delta T \\ \varepsilon_y - \alpha_y \Delta T \\ \gamma_{xy} - \alpha_{xy} \Delta T \\ \gamma_{yz} \\ \gamma_{zx} \end{Bmatrix} \tag{3}$$

where Q'_{ij}, α_x, α_y and α_{xy} are respectively the reduced stiffness coefficients and the thermal expansion coefficients of the lamina in the x-y-z system, which are obtained using the following expressions:

$$\begin{aligned}
Q'_{11} &= Q_{11}c^4 + 2(Q_{12} + 2Q_{66})c^2s^2 + Q_{22}s^4 \\
Q'_{12} &= (Q_{11} + Q_{22} - 4Q_{66})c^2s^2 + Q_{12}(c^4 + s^4) \\
Q'_{16} &= -Q_{22}cs^3 + Q_{11}c^3s - (Q_{12} + 2Q_{66})cs(c^2 - s^2) \\
Q'_{22} &= Q_{11}s^4 + 2(Q_{12} + 2Q_{66})c^2s^2 + Q_{22}c^4 \\
Q'_{26} &= -Q_{22}c^3s + Q_{11}cs^3 + (Q_{12} + 2Q_{66})cs(c^2 - s^2) \\
Q'_{66} &= (Q_{11} + Q_{22} - 2Q_{66})c^2s^2 + Q_{66}(c^2 - s^2)^2 \\
Q'_{44} &= Q_{44}c^2 + Q_{55}s^2 \\
Q'_{45} &= (-Q_{44} + Q_{55})cs \\
Q'_{55} &= Q_{44}s^2 + Q_{55}c^2 \\
\alpha_x &= \alpha_1 c^2 + \alpha_2 s^2 \\
\alpha_y &= \alpha_1 s^2 + \alpha_2 c^2 \\
\alpha_{xy} &= 2(\alpha_1 - \alpha_2)cs
\end{aligned} \tag{4}$$

in which c=cosθ and s=sinθ with θ representing the angle between the axes 1 and x, while z axis is assumed to coincide with axis 3.

3. Higher-order shear deformation theory

The higher-order shear deformation theory developed by Reddy (1984) accounts for:

(1) the transverse shear deformation;
(2) the parabolic variation of the transverse shear strain throughout the thickness of the plate;
(3) the vanishing shear stresses on the plate surfaces. This theory yields the following displacement field:

$$u = u_0 + z\,\psi_x - \frac{4}{3h^2}z^3\left(\psi_x + \frac{\partial w}{\partial x}\right)$$

$$v = v_0 + z\psi_y - \frac{4}{3h^2}z^3(\psi_y + \frac{\partial w}{\partial y})$$
$$w = w(x, y) \tag{5}$$

where u and v are the inplane displacements at any point (x, y, z), u_0 and v_0 denote the inplane displacements of the point (x, y, 0) on the midplane, w is the deflection and is assumed to be constant in the thickness direction z, ψ_x and ψ_y are the rotations of the normals to the midplane about the y and x axes, respectively, and h denotes the thickness of the plate.

As indicated by Reddy, this theory employs the same number of degrees of freedom as those of the first order shear deformation theory but gives more accurate results, especially for the thick plates with the length-to-thickness ratio lower than a/h=10.

4. Finite strip method

In the present analysis, the rectangular composite laminate is modeled by a number of finite strips, each of which has 3 equally spaced nodal lines (Fig. 1).

For the laminates with two simply supported opposite sides, the boundary conditions at both ends of the strip are

$$w = \psi_x = 0, \quad M_y = 0, \quad N_y = N_{xy} = 0 \quad at \quad y = 0 \quad \text{and} \quad y = l \tag{6}$$

In this case, the midplane displacements and the normal rotations can be expressed in terms of the above displacement parameters as

$$u_0 = \sum_{m=1}^{r}\sum_{i=1}^{3}[N_i(x)u_{im}\sin\frac{m\pi y}{l} + N_i(x)\bar{u}_{im}\cos\frac{m\pi y}{l}]$$
$$v_0 = \sum_{m=1}^{r}\sum_{i=1}^{3}[N_i(x)v_{im}\cos\frac{m\pi y}{l} + N_i(x)\bar{v}_{im}\sin\frac{m\pi y}{l}]$$
$$w = \sum_{m=1}^{r}\sum_{i=1,3}[F_i(x)w_{im} + H_i(x)(\frac{\partial w}{\partial x})_{im}]\sin\frac{m\pi y}{l}$$
$$\psi_x = \sum_{m=1}^{r}\sum_{i=1}^{3}N_i(x)\psi_{xim}\sin\frac{m\pi y}{l}$$
$$\psi_y = \sum_{m=1}^{r}\sum_{i=1}^{3}N_i(x)\psi_{yim}\cos\frac{m\pi y}{l} \tag{7}$$

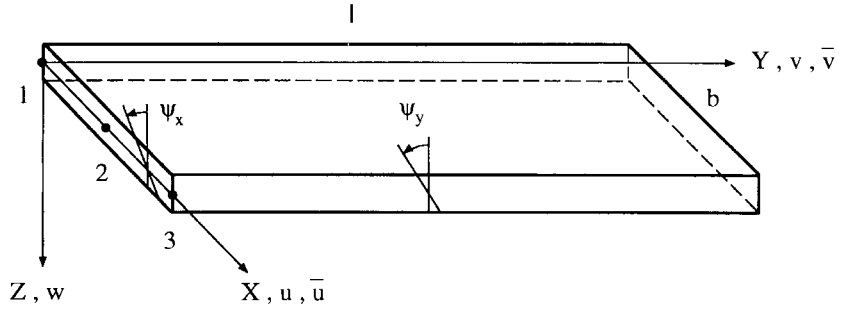

Fig. 1 A finite strip

where r is the number of harmonics employed in the analysis; l is the length of the strip; u_{im}, $\overline{u}_{im}$, v_{im}, $\overline{v}_{im}$, w_{im}, $(\partial w/\partial x)_{im}$, ψ_{xim} and ψ_{yim} are the displacement parameters for nodal line i and the mth harmonic; $N_i(x)$ is the quadratic Lagrangian interpolation function for nodal line i (i=1 to 3) and has the following form:

$$N_i(x) = \prod_{\substack{j=1 \\ j\neq i}}^{3} \frac{x - x_j}{x_i - x_j} \tag{8}$$

$F_i(x)$ and $H_i(x)$ (i=1,3) are the following Hermitian cubic polynomials:

$$\begin{aligned} F_1(x) &= 1 - 3(\frac{x}{b})^2 + 2(\frac{x}{b})^3 \\ F_3(x) &= 3(\frac{x}{b})^2 - 2(\frac{x}{b})^3 \\ H_1(x) &= x[1 - 2\frac{x}{b} + (\frac{x}{b})^2] \\ H_3(x) &= x[(\frac{x}{b})^2 - \frac{x}{b}] \end{aligned} \tag{9}$$

in which b is the width of the strip.

Substituting Eq. (7) into Eq. (5), the displacements at any point (x, y, z) within the strip can be interpolated as follows:

$$\{f\} = [u, v, w]^T = \sum_{m=1}^{r} \sum_{i=1}^{3} [N]_{im} \{\delta\}_{im} \tag{10}$$

where

$$\{\delta\}_{im} = \begin{cases} [u_{im}, \overline{u}_{im}, v_{im}, \overline{v}_{im}, w_{im}, (\dfrac{\partial w}{\partial x})_{im}, \psi_{xim}, \psi_{yim}]^T & \text{for } i = 1,3 \\ [u_{im}, \overline{u}_{im}, v_{im}, \overline{v}_{im}, \psi_{xim}, \psi_{yim}]^T & \text{for } i = 2 \end{cases} \tag{11}$$

$[N]_{im}$ is the interpolation matrix. For i=1 or 3, it is written as

$$[N]_{im} = \begin{bmatrix} N_i S_m & N_i C_m & 0 & 0 & -az^3 F'_i S_m & -az^3 H'_i S_m & (z - az^3) N_i S_m & 0 \\ 0 & 0 & N_i C_m & N_i S_m & -az^3 k_m F_i C_m & -az^3 k_m H_i C_m & 0 & (z - az^3) N_i C_m \\ 0 & 0 & 0 & 0 & F_i S_m & H_i S_m & 0 & 0 \end{bmatrix} \tag{12}$$

in which S_m=sin$k_m y$, C_m=cos$k_m y$, and $k_m = m\pi/l$; $(\,)' = \dfrac{d(\,)}{dx}$ and $(\,)'' = \dfrac{d^2(\,)}{dx^2}$; $a = 4/3h^2$. For i=2, the above expression is applicable without the fifth and the sixth columns.

The following strain-displacement relationships are used in the analysis:

$$\varepsilon_x = \frac{\partial u}{\partial x}$$

$$\varepsilon_y = \frac{\partial v}{\partial y}$$
$$\gamma_{xy} = \frac{\partial u}{\partial y} + \frac{\partial v}{\partial x}$$
$$\gamma_{yz} = \frac{\partial v}{\partial z} + \frac{\partial w}{\partial y}$$
$$\gamma_{zx} = \frac{\partial u}{\partial z} + \frac{\partial w}{\partial x} \tag{13}$$

By substituting Eq. (10) into Eq. (13), the strain vector can be expressed in terms of the displacement parameters as

$$\{\varepsilon\} = [\varepsilon_x, \varepsilon_y, \gamma_{xy}, \gamma_{yz}, \gamma_{zx}]^T = \sum_{m=1}^{r} \sum_{i=1}^{3} [B]_{im} \{\delta\}_{im} \tag{14}$$

where $[B]_{im}$ is the strain matrix. For i=1 or 3, $[B]_{im}$ has the following expression:

$$[B]_{im} = \begin{bmatrix} N_i'S_m & N_i'C_m & 0 & 0 & -az^3F_i''S_m \\ 0 & 0 & -k_mN_iS_m & k_mN_iC_m & k_m^2az^3F_iS_m \\ k_mN_iC_m & -k_mN_iS_m & N_i'C_m & N_i'S_m & -2k_maz^3F_i'C_m \\ 0 & 0 & 0 & 0 & k_m(1-3az^2)F_iC_m \\ 0 & 0 & 0 & 0 & (1-3az^2)F_i'S_m \end{bmatrix}$$

$$\begin{bmatrix} -az^3H_i''S_m & (z-az^3)N_i'S_m & 0 \\ k_m^2az^3H_iS_m & 0 & -k_m(z-az^3)N_iS_m \\ -2k_maz^3H_i'C_m & k_m(z-az^3)N_iC_m & (z-az^3)N_i'C_m \\ k_m(1-3az^2)H_iC_m & 0 & (1-3az^2)N_iC_m \\ (1-3az^2)H_i'S_m & (1-3az^2)N_iS_m & 0 \end{bmatrix} \tag{15}$$

For i=2, the above expression is valid without the fifth and the sixth columns.

From Eq. (15) it can be observed that γ_{yz} and γ_{zx} vary proportionally to $(1-3az^2)$ throughout the thickness of the plate, and $\gamma_{yz}=\gamma_{zx}=0$ at $z=\pm h/2$ which leads to $\tau_{yz}=\tau_{zx}=0$ at the top and the bottom surfaces of the plate.

The stiffness matrix of the strip can be formed by following the procedure commonly used in the finite strip analysis (see Cheung *et al.* 1996). The submatrix corresponding to nodal lines i and j can be evaluated as follows:

$$[K]_{ijmn} = \int_h \int_l \int_b [B]_{im}^T [Q'][B]_{jn} dx\, dy\, dz \tag{16}$$

where m and n denote the related series terms, $[Q']$ is the elastic matrix in Eq. (3).

The integrations in the above equations can be implemented analytically in the y and z directions, and the following expressions can be employed

$$I_1 = \int_l \sin k_m y \sin k_n y dy = \begin{cases} \frac{l}{2} & \text{for } m=n \\ 0 & \text{for } m \neq n \end{cases}$$

$$I_2 = \int_l \cos k_m y \cos k_n y dy = \begin{cases} \frac{l}{2} & \text{for } m=n \\ 0 & \text{for } m \neq n \end{cases}$$

$$I_3 = \int_l \sin k_m y \cos k_n y dy = \begin{cases} \frac{2ml}{\pi(m^2-n^2)} & \text{for } m-n=2k+1 \\ 0 & \text{for } m-n=2k \\ & (k=0, 1, 2 \cdots) \end{cases} \tag{17}$$

In order to eliminate the 'shear locking' of the thin plates, in calculating the transverse shear stiffness, the reduced integration technique (see Cook *et al.* 1989), i.e., the two point Gaussian quadrature, is used in the x direction.

Because the integral I_3 does not always vanish for $m \neq n$, different series terms are generally coupled in the analysis. However, for some laminates, e.g., cross-ply or anti-symmetrical angle-ply laminates, all the stiffness coefficients associated with I_3 disappear. Consequently, the different series terms become uncoupled and the efficiency of the analysis is enhanced significantly.

The thermal load vector for the m-th harmonic and the i-th nodal line is

$$\{P_t\}_{im} = \int_h \int_l \int_b [B]_{im}^T [Q'] \{\alpha_x \Delta T, \alpha_y \Delta T, \alpha_{xy} \Delta T, 0, 0\}^T dxdydz \tag{18}$$

After assembling the above strip matrices over the entire structure, the prebuckling thermal analysis is carried out by solving the following matrix equation for the unknown displacements $\{\delta\}$:

$$[K]\{\delta\} = \{P_t\} \tag{19}$$

Then, the initial thermal inplane stresses are evaluated using Eq. (14) and Eq. (3). Furthermore, the geometrical matrix (see Dawe and Roufaeil 1982) can be formed as:

$$[L]_{ijmn} = \int_h \int_l \int_b ([G_u]_{im}^T [\sigma^o][G_u]_{jn} + [G_v]_{im}^T [\sigma^o][G_v]_{jn} + [G_w]_{im}^T [\sigma^o][G_w]_{jn}) dxdydz \tag{20}$$

where $[G_u]_{im}$, $[G_v]_{im}$ and $[G_w]_{im}$ are matrices defined by

$$\left[\frac{\partial u}{\partial x}, \frac{\partial u}{\partial y}\right]^T = \sum_{m=1}^{r} \sum_{i=1}^{3} [G_u]_{im} \{\delta\}_{im}$$

$$\left[\frac{\partial v}{\partial x}, \frac{\partial v}{\partial y}\right]^T = \sum_{m=1}^{r} \sum_{i=1}^{3} [G_v]_{im} \{\delta\}_{im}$$

$$\left[\frac{\partial w}{\partial x}, \frac{\partial w}{\partial y}\right]^T = \sum_{m=1}^{r} \sum_{i=1}^{3} [G_w]_{im} \{\delta\}_{im} \tag{21}$$

$[\sigma^o]$ is the matrix of initial thermal inplane stresses:

$$[\sigma^o] = \begin{bmatrix} \sigma_x^o & \tau_{xy}^o \\ \tau_{xy}^o & \sigma_y^o \end{bmatrix} \tag{22}$$

Thereafter, the initial thermal buckling behavior can be revealed by solving the following eigenvalue matrix equation:

$$[K]\{\bar{\delta}\} + \lambda[L]\{\bar{\delta}\} = \{0\} \tag{23}$$

The product of λ and the initial guessed value ΔT is the critical thermal buckling temperature T_{cr}.

5. Results and discussion

If a laminated composite plate with symmetrical lay-ups is subjected to a temperature rise which is distributed uniformly across the thickness, the prebuckling deflections do not occur. However, as the temperature keeps rising, the thermal stresses build up in the plate and eventually cause the plate to buckle. The thermal buckling also happens in simply supported antisymmetrical angle-ply laminates under some types of temperature change. In the present study, the thermal buckling analyses of the simply supported rectangular symmetrical cross-ply, symmetrical and antisymmetrical angle-ply laminates are carried out using the proposed approach. The thermal loading is restricted to uniform temperature rise though this approach can also be applied to other types of temperature distribution. The effects of several parameters, such as aspect ratio, length-to-thickness ratio, number of plies, fibre orientation and stacking sequence on the critical temperature are investigated.

In the following analyses, unless indicated otherwise, the lamina properties are assumed to be:

$$E_1 = 181.0E_0 \quad E_2 = 10.3E_0$$
$$G_{12} = 7.17E_0 \quad G_{23} = 2.39E_0 \quad G_{31} = 5.98E_0$$
$$\nu_{12} = 0.28 \quad \alpha_1 = 0.02\alpha_0 \quad \alpha_2 = 22.5\alpha_0$$

where E_0 and α_0 represent arbitrary reference values.

For a beam with rectangular cross-section under axial compression, the critical buckling stress is proportional to h^2/a^2 where h and a are respectively the depth and the length of the beam. If the compression is caused by a temperature rise, the critical stress is also proportional to $\alpha_o T_{cr}$. This leads to: $\sigma_{cr}=k_1h^2/a^2=k_2\alpha_o T_{cr}$ or $\alpha_o T_{cr}a^2/h^2=k_1/k_2=constant$ with k_1 and k_2 denoting the related factors of proportion. This relationship is also valid for thin plates (Johns 1995). However, for thick plates, the transverse shear deformation reduces the stiffness of the structure significantly. As a result, the dimensionless critical temperature $\alpha_o T_{cr}a^2/h^2$ decreases as the plate becomes relatively thicker and the a/h ratio goes down. This trend can be observed in the following analyses.

5.1. Simply supported rectangular (0°/90°/90°/0°) laminates

A rectangular laminate is constructed from four equal thickness layers oriented at (0°/90°/90°/0°), and subjected to a uniform temperature rise. The thickness of the plate is h, the side lengths are a in the x direction and b in the y direction. The four edges of the plate are hinged and immovable in all the inplane directions. Therefore, the prebuckling deformation is restrained and the initial thermal stresses can be evaluated from Eq. (3) with all the strains being equal to zero.

In the analysis, the entire plate is divided into four strips parallel to the longer sides. One longitudinal harmonics is taken for b/a=1, and two for b/a>1. Further increasing the number of

strips and series terms makes only little improvement.

The resulting dimensionless critical temperature is shown in Table 1 as the function of the length-to-thickness ratio a/h and the aspect ratio b/a. The results show that the transverse shear deformation reduces the critical temperature significantly. As the length-to-thickness ratio a/h changes from 50 to 4, the dimensionless critical temperature reduces about 70 percent. By contrast, the aspect ratio b/a has only little influence on the critical temperature. For a given a/h, only 5 percent fluctuation can be detected within the range of $1.0 \leq b/a \leq 2.0$.

5.2. Simply supported antisymmetric angle-ply laminates

A square laminate of side length a and thickness h is made up of even number of equal thickness layers oriented at $(\theta^\circ/-\theta^\circ \cdots)$, and subjected to a uniform temperature rise. Its four edges are hinged and free in the tangential inplane direction but immovable in the normal inplane direction. It can be proved that in this case there is no prebuckling deformation, and the initial inplane thermal stresses can be computed using Eq. (3) with all the strain components assumed to be zero (see Wu and Tauchert 1980).

In the analysis, the entire plate is divided into four strips, and only one longitudinal harmonic is required.

The resulting dimensionless critical temperature is shown in Table 2 as the function of the length-to-thickness ratio, the number of plies and the angle θ. For $\theta=45^\circ$, the effect of the plate thickness is depicted in Fig. 2 in comparison with the solutions based on the first order shear deformation theory (FSDT) and the classical thin plate theory (CPT) (FSDT and CPT results are simply scaled off Fig. 3 of Tauchert 1987). It can be seen from this figure that the classical thin plate theory overestimates the critical temperature for thick and moderately thick plates, the significant error can be detected for the laminates with $a/h<25$. The first order shear deformation theory yields the satisfactory results for the thin and moderately thick laminates. However, for the thick laminates with $a/h=4$, that theory also overestimates the critical temperature. For instance, for eight-ply laminate of $a/h=4$, FSDT solution is 0.323 but the present result is 0.272. This means that for thick plates the error of the first order shear deformation theory may reach eighteen percent in comparison with the higher order theory.

5.3. Simply supported symmetric angle-ply square laminates

A square laminate of side length a and thickness h is made up of odd number of equal thickness layers oriented at $(\theta^\circ/-\theta^\circ \cdots)$, and subjected to a uniform temperature rise. Its four edges are hinged and fixed in all the inplane directions. Because the prebuckling deformation is

Table 1 Critical temperature of rectangular (0/90/90/0) laminate

a/h	$\alpha_0 T_{cr} a^2/h^2$				
	$\bar{b}/a$=1.0	$\bar{b}/a$=1.25	$\bar{b}/a$=1.5	$\bar{b}/a$=1.75	$\bar{b}/a$=2.0
4	0.1841	0.1826	0.1859	0.1891	0.1841
10	0.4303	0.4458	0.4496	0.4322	0.4303
20	0.5553	0.5818	0.5716	0.5534	0.5553
50	0.6071	0.6382	0.6219	0.6035	0.6071

Table 2 Critical temperature of square (θ/-θ···) laminate

a/h	No. of Plies	$\alpha_o T_{cr} a^2/h^2$			
		θ=0°	θ=15°	θ=30°	θ=45°
4	2	0.2164	0.2013	0.1984	0.2022
	4	0.2164	0.2273	0.2472	0.2550
	8	0.2164	0.2369	0.2627	0.2717
10	2	0.4705	0.3848	0.3490	0.3541
	4	0.4705	0.5019	0.5871	0.6296
	8	0.4705	0.5321	0.6444	0.6948
20	2	0.5727	0.4486	0.3967	0.4025
	4	0.5727	0.6133	0.7388	0.8068
	8	0.5727	0.6547	0.8229	0.9056
50	2	0.6105	0.4711	0.4130	0.4190
	4	0.6105	0.6547	0.7974	0.8770
	8	0.6105	0.7006	0.8932	0.9910

restrained, the initial inplane thermal stresses can be obtained in the same methods as in the previous examples.

A variety of strip divisions combined with different numbers of series terms is employed for the analysis. The convergency is presented in Table 3 for (45°/-45°/45°) laminate of a/h=10. It can be observed that the resulting critical temperature is reduced drastically at beginning and becomes steady later on as the number of strips and the number of series terms both increase

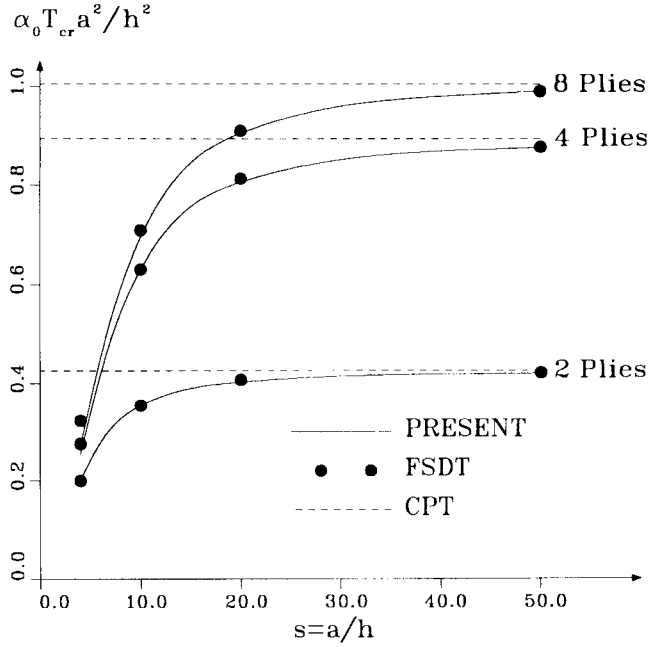

Fig. 2 Square antisymmetric laminates θ=45°

simultaneously. It can also be seen that dividing the entire plate into eight equal strips and using eight series terms will yield reasonably accurate solutions. The consequent values for dimensionless critical temperature are documented in Table 4 as the function of the length-to-thickness ratio, the number of plies and the angle θ. The results based on the classical plate theory (CPT) (scaled off Fig. 4 of Tauchert and Huang 1987) are also listed in the same table for comparison. It can be noticed that the present method and the thin plate theory yield almost the same results for the thin laminates (a/h=100). However, the thin plate theory overestimates the critical temperature for moderately thick and thick laminates. The error reaches more than thirty percent for a/h=10 and more than seventy percent for a/h=4 in comparison with the present analysis.

6. Conclusions

In the present study, the thermal buckling analysis of thick anisotropic laminated composite plates is carried out using the finite strip method based on the higher-order shear deformation theory. This theory accounts for the parabolic distribution of the transverse shear strains through the thickness of the plate and for zero transverse shear stresses on the plate surfaces. Therefore, this theory yields improved results over the Mindlin plate theory and eliminates the need for shear

Table 3 Convergency for (45/-45/45) laminate of a/h=10

No. of strips	2	3	4	5	6	7	8	9
No. of terms	2	3	4	5	6	7	8	9
$\alpha_0 T_{cr} a^2/h^2$	0.5572	0.4812	0.4686	0.4614	0.4561	0.4533	0.4500	0.4487

Table 4 critical temperature of square (θ/-θ···) laminate

a/h	No. of Plies	$\alpha T_{cr} a^2/h^2$				
		θ=0°	θ=11.25°	θ=22.5°	θ=33.75°	θ=45°
4	1	0.1245	0.1260	0.1256	0.1252	0.1241
	3	0.1245	0.1323	0.1535	0.1845	0.1964
	9	0.1245	0.1375	0.1733	0.2310	0.2592
10	1	0.2935	0.3023	0.3217	0.3172	0.3160
	3	0.2935	0.3166	0.3840	0.4383	0.4500
	9	0.2935	0.3563	0.5195	0.6544	0.6815
20	1	0.3654	0.3823	0.4222	0.4052	0.4073
	3	0.3654	0.4021	0.5078	0.5493	0.5674
	9	0.3654	0.4609	0.7314	0.8492	0.8956
100	1	0.3976	0.4193	0.4716	0.4465	0.4534
	3	0.3976	0.4421	0.5710	0.6015	0.6264
	9	0.3976	0.5106	0.8036	0.9409	0.9988
CPT	1	0.400	0.422	0.489	0.477	0.479
	3	0.400	0.442	0.593	0.629	0.654
	∞	0.400	0.521	0.888	0.984	1.050

correction factors in calculating the transverse shear stiffness.

The effects of some structural parameters such as aspect ratio, length-to-thickness ratio, number of plies, fibre orientation and stacking sequence on critical temperature are investigated. It is found that for the very thick laminates of a/h=4, the transverse shear deformation reduces the critical temperature about seventy percent. For such the laminates the first order shear deformation theory also overestimates the critical temperature. In some cases the error reaches eighteen percent in comparison with the higher order shear deformation analysis.

Acknowledgements

The financial supports from the Department of National Defence and the Natural Sciences and Engineering Research Council of Canada are gratefully acknowledged.

References

Agarwal, B.D. and Broutman, L.J. (1980). *Analysis and Performance of Fiber Composites.* John-Wiley & Sons, New York.

Chen, L.W. & Chen, L.Y. (1987,. "Thermal buckling of laminated cylindrical plates", *Composite Struct.* **8**, 189-205.

Cheung, M.S., Li, W. and Chidiac, S.E. (1996). *Finite Strip Analysis of Bridges*, E & FN SPON, London.

Cook, R.D., Malkus, D.S. and Plesha, M.E. (1989). *Concepts and Applications of Finite Element Analysis*, 3rd edt. John Wiley & Sons, New York.

Dawe, D.J. and Roufaeil, O.L. (1982), "Buckling of rectangular Mindlin plates", *Computers & Structures*, **15**(4), 461-471.

Johns, D.J. (1995). *Thermal Stress Analyses*, Pergamon Press Ltd, Oxford.

Reddy, J.N. (1984), "A simple higher-order theory for laminated composite plates", *Journal of Applied Mechanics*, **51**, 745-752.

Reddy, J.N. and Phan, N.D. (1985), "Stability and vibration of isotropic, orthotropic and laminated plates according to a higher-order shear deformation theory", *Journal of Sound and Vibration*, **98**(2), 157-170.

Shu, X. and Sun, L. (1994), "Thermomechanical buckling of laminated composite plates with higher-order transverse shear deformation", *Computers & Structures*, **53**(1), 1-7.

Stavsky, Y. (1975), "Thermoelastic stability of laminated orthotropic circular plates", *Acta Mech.*, **22**, 31-51.

Tauchert, T.R. (1987), "Thermal buckling of thick antisymmetric angle-ply laminates", *Journal of Thermal Stresses*, **10**(2), 113-124.

Tauchert, T.R. and Huang, N.N. (1986), "Thermal buckling and postbuckling behavior of antisymmetric angle-ply laminates", *Proc. Int. Symp. Composite Material and Structures*, Beijing, June 1986, 357-362.

Tauchert, T.R. and Huang, N.N. (1987), "Thermal buckling of symmetric angle-ply laminated plates", *Composite Structures* 4, 1, Edited by I. H. Marshall, 1.424-1.435, Elsevier Applied Science, London & New York.

Whitney, J.M. and Ashton, J.E. (1971), "Effect of environment on the elastic response of layered composite plate", *AIAAJ.* **7**, 1708-1713.

Wu, C.H. and Tauchert, T.R. (1980), "Thermoelastic analysis of laminated plates, 2. antisymmetric cross-ply and angle-ply laminates", *Journal of Thermal Stresses*, **3**, 365-378.